

Experimental Fluid Mechanics

Klaus Hufnagel

Wind Tunnel Balances

 Springer

Experimental Fluid Mechanics

Series Editors

Cameron Tropea, Technische Universität Darmstadt, Darmstadt, Hessen, Germany

David Rival, Department of Mechanical and Materials Engineering, Queen's University, Kingston, ON, Canada

More information about this series at <https://link.springer.com/bookseries/3837>

Klaus Hufnagel

Wind Tunnel Balances

 Springer

Klaus Hufnagel
Wind Tunnel
Technische Universität Darmstadt
Darmstadt, Germany

ISSN 1613-222X

ISSN 2197-9510 (electronic)

Experimental Fluid Mechanics

ISBN 978-3-030-97765-8

ISBN 978-3-030-97766-5 (eBook)

<https://doi.org/10.1007/978-3-030-97766-5>

© The Editor(s) (if applicable) and The Author(s), under exclusive license to Springer Nature Switzerland AG 2022

This work is subject to copyright. All rights are solely and exclusively licensed by the Publisher, whether the whole or part of the material is concerned, specifically the rights of translation, reprinting, reuse of illustrations, recitation, broadcasting, reproduction on microfilms or in any other physical way, and transmission or information storage and retrieval, electronic adaptation, computer software, or by similar or dissimilar methodology now known or hereafter developed.

The use of general descriptive names, registered names, trademarks, service marks, etc. in this publication does not imply, even in the absence of a specific statement, that such names are exempt from the relevant protective laws and regulations and therefore free for general use.

The publisher, the authors and the editors are safe to assume that the advice and information in this book are believed to be true and accurate at the date of publication. Neither the publisher nor the authors or the editors give a warranty, expressed or implied, with respect to the material contained herein or for any errors or omissions that may have been made. The publisher remains neutral with regard to jurisdictional claims in published maps and institutional affiliations.

This Springer imprint is published by the registered company Springer Nature Switzerland AG
The registered company address is: Gewerbestrasse 11, 6330 Cham, Switzerland

I would like to dedicate this book to Prof. Bernd Ewald, who was my teacher and doctoral advisor. From him, I acquired most of the knowledge in the field of wind tunnel balances. In the beginning of the 1980s, I was hired by him for a research project with the aim to develop internal balances for the emerging cryogenic wind tunnels. He was aware that the very promising aim of having the same Reynolds number in a wind tunnel test as on subsonic cruise flight could not be achieved without a force measuring technique that has the same accuracy as the systems built for conventional tunnels. The project was successfully brought to completion, but there was no interest in the industry to take over this knowledge of cryogenic balances for industrial production, and so, he decided to offer such balances directly from the university. He was an engineer that showed us how engineering creativity could solve totally new problems when it is coupled with solid engineering knowledge and art. He analyzed lot of problems by simple models and so delivered

the basis and the direction for the knowledge transfer to practical applications. His impact on the development on present status of wind tunnel balances is documented in numerous papers, the study of which is highly recommended if somebody wants to enter this field. Prof. Ewald passed away in June 2019.

Preface

The motivation to write this book came to me while sorting out material which the head of our institute, Prof. Bernd Ewald, had produced and collected on the subject of balances during his career. Following his retirement in 1998, he continued to work on balance design, and although he had intended on summarizing his life experience with balances in the form of a book, he became side-tracked—he dedicated his time to rebuilding a famous flying wing aircraft, the Horton IV. On every visit to the office, he therefore brought with him a trunk full of wind tunnel balance documents, rather than throwing them away. Together with the documentation I had collected at this time over my own 15 years of working with balances, I was therefore faced with deciding the fate of all this accumulated knowledge. The documentation comprised over six hundred articles related to wind tunnel balances and calibration machines and addressed such issues as operation over a wide temperature range or under large temperature gradients. Especially while reading through Prof. Ewald's notes, it became clear to me that we had overcome innumerable design problems in the past that represented important solutions and experience that others could benefit from.

It eventually became apparent that the only solution to preserving this knowledge for future reference was to write a book, condensing this combined experience obtained over a period of 36 years. Although I started this endeavor well in advance of my own retirement, this 14 year lead time was still not sufficient to finish the project. It was also never evident to me whether the book would be outdated before publication. The eventual role of computational fluid dynamics (CFD) was and is still not clear—to what extent wind tunnel testing would remain an important design tool for the aviation industry? In comparison with complicated and costly experiments employing contemporary techniques such as particle image velocimetry (PIV) or pressure/temperature sensitive paints (PSP/TSP), CFD appeared in many respects to be advantageous. However, in the end, both CFD and wind tunnel can be viewed as aerodynamic simulation tools that have their own specific uncertainties in the prediction of the airflow around an airplane. Since the development of cryogenic wind tunnels, which are able to close the Reynolds number gap between model testing and reality, wind tunnel testing now delivers extremely precise data for the performance of an airplane. So, time has revealed that wind tunnel balances remain

an important tool in the overall design of aircraft, and therefore, it is my hope that this book will be of use to present and future generations of engineers and technicians dealing with this measurement technology.

Darmstadt, Germany
April 2021

Klaus Hufnagel

Acknowledgements Writing a book is a one part of the story, the other is to get it published. First, I have to thank my longtime colleague Matthias Quade for the first review of the text. For bringing the book to a scientific standard, I want to thank very much Prof. Dr.-Ing Cameron Tropea for the time he spent in proofreading and his support in the layout of the book. Finally, I would like to extend a word of thanks to numerous of my colleagues throughout the world, who have graciously sent me pictures of their balances and instruments and allowed me to use them in this book.

Contents

1	Historical Review	1
1.1	Introduction	1
1.2	From Fundamental Physics to the First Force Transducers	1
1.3	Force Measurement in Wind Tunnels	6
	References	10
2	Basics	11
2.1	Basics of Wind Tunnel Balance System	12
2.2	Basic Terms of Balance Metrology	13
2.3	Definition of Axis Systems	18
2.4	Signal Conventions	19
2.5	Relevant Wind Tunnel Standards	20
	References	21
3	Balance Types	23
3.1	External Balances	23
3.1.1	Weigh Beam Balances	26
3.1.2	Pyramidal Balance	28
3.1.3	Platform Balance	30
3.1.4	Coaxial Balances	32
3.1.5	Yoke Balance	35
3.1.6	Spiral Spring Type Balance	37
3.1.7	Half Model and Side Wall Balances	37
3.1.8	Three-Flange Balance	38
3.2	Internal Balances	38
3.2.1	Sting Balances	40
3.2.2	Box Balances	43
3.2.3	Floating Frame Balances	44
3.2.4	Rotating Balances	45
3.2.5	Hinge Moment Balances	48
3.2.6	Rudder Balances	48
3.2.7	Missile Balances	48

3.3	Magnetic Suspension Balances	48
3.4	Electromagnetic Balances	49
	References	51
4	Model Mounting	53
4.1	Mounting of Models to External Balances	55
4.2	Mounting Models to Internal Balances	57
4.3	Correction of Mounting and Balance Elasticity	58
4.3.1	Correction by Sting Deformation Measurement	60
4.3.2	Correction by Model Position Measurement	61
4.3.3	Correction of Vibration by Active Sting Damping	61
4.4	Internal Balance Joints	61
4.4.1	Cone	64
4.4.2	Cylinder	70
4.4.3	Bloc	72
4.4.4	Flange	73
4.4.5	Summary Balance Joints	77
4.4.6	Adapters for the Use of Internal Balances as Box Balances and Vice Versa	78
	References	79
5	Specification	81
5.1	Definition of Load	83
5.2	Specification of Balance Load Ranges	83
5.3	Dynamic Loads	88
5.4	Maximum Combined Load; Maximum Single Load	88
5.5	Safety Factors	89
5.6	Deflections	90
5.7	Constraints Due to Model Design (Space and Position)	90
5.8	Specific Load Parameter	91
5.9	Principle Design Equations (Feasibility)	92
5.10	Specification of Resolution, Repeatability and Sensitivities	94
5.10.1	Resolution	94
5.10.2	Repeatability	94
5.10.3	Sensitivity	95
5.11	Specification of Uncertainty	95
5.12	Specification of Thermal Characteristics	96
5.12.1	Operating Temperature Range	97
5.12.2	Zero Drift	98
5.12.3	Sensitivity Drift	98
5.12.4	Temperature Gradients	99
5.13	Balance Interfaces	99
5.14	Miscellaneous Specifications	100
5.14.1	Reference Planes and Reference Point	100
5.14.2	Moisture Protection	101
	References	101

- 6 Design of Balances** 103
 - 6.1 Internal Balances 103
 - 6.1.1 Moment and Force Separation Basic Design
Equation 104
 - 6.1.2 Specific Load Parameter 110
 - 6.1.3 Routine Design Methods for Internal Balances 110
 - 6.1.4 Design of Solid Bending Section of Internal
Balances 123
 - 6.1.5 Design of Cage Bending Section 125
 - 6.1.6 Design of Axial Force Section 133
 - 6.2 External Balances 152
 - 6.2.1 Load Cells and Load Cell Arrangement 153
 - 6.2.2 Weighbridge 155
 - 6.2.3 Connecting Rods and Flexures 156
 - 6.2.4 Temperature Problems of External Balances 157
 - 6.3 Semi-span Balances 158
 - 6.3.1 Thermal Problems of Semi-span Balances 163
 - 6.4 Bridging 167
 - 6.4.1 Model Data Bridging 169
 - 6.4.2 Air Supply Bridging 169
 - 6.5 Life Time and Fatigue Calculations 171
 - 6.5.1 Determination of the Wöhler-Curve (S-N-Curve) 173
 - 6.5.2 Stress Collective 173
 - 6.5.3 Linear Damage Accumulation (Miner Rule) 174
 - 6.5.4 Summary 175
 - References 176
- 7 Balance Material and Fabrication Methods** 177
 - 7.1 Balance Material 177
 - 7.2 Material Characteristics 178
 - 7.2.1 Tensile Strength and Yield Strength 178
 - 7.2.2 Dynamic Stability and Fracture Toughness 179
 - 7.2.3 Young’s Module 179
 - 7.2.4 Thermal Expansion Coefficient 180
 - 7.2.5 Hysteresis 180
 - 7.2.6 Creep 180
 - 7.2.7 Heat Treatment 180
 - 7.3 Maraging Steels 181
 - 7.3.1 Heat Treatment of Maraging Steels 182
 - 7.4 Stainless Steels 183
 - 7.4.1 Heat Treatment of Stainless Steels 183
 - 7.5 Copper Beryllium 183
 - 7.5.1 Heat Treatment of Copper-Beryllium 184
 - 7.6 Titanium Alloys 184
 - 7.6.1 Heat Treatment of TiAl6V4 185

- 7.7 Aluminum Alloys 185
 - 7.7.1 Heat Treatment of Aluminum Alloys 185
- 7.8 Balance Body Fabrication Methods 186
- 7.9 One Piece Fabrication 186
- 7.10 Multi-component Balances 187
- 7.11 Surface Protection 187
- References 188
- 8 Strain Measurement 189**
 - 8.1 Strain Gauge 189
 - 8.1.1 Wire Strain Gauge Fundamentals 189
 - 8.1.2 Semiconductor Strain Gauge Fundamentals 191
 - 8.1.3 Fiber Optic Strain Gauge Fundamentals 193
 - 8.2 Strain Gauge Selection 198
 - 8.3 Strain Gauge Application 199
 - 8.3.1 Bonding 200
 - 8.4 Wheatstone Bridge Wiring 200
 - 8.4.1 Notation of Gauging and Wiring 202
 - 8.4.2 Relation Between Signal and Resistance 202
 - 8.4.3 Electrical Influence of Bridge Wires 203
 - 8.4.4 Mechanical Influence of Bridge Wiring 204
 - 8.5 Compensation of Bridge Zero Output 206
 - 8.6 Compensation of Thermal Effects 206
 - 8.6.1 Compensation of Zero Drift for Metal Foil Strain Gauges 206
 - 8.6.2 Compensation of Sensitivity Shift of Metal Foil Strain Gauges 211
 - 8.6.3 Computational Correction Methods of Temperature Effects 214
 - 8.7 Direct Read Balance Wiring 215
 - 8.8 Moment Balance Wiring 216
 - 8.9 Insulation and Moisture Proofing 217
 - 8.10 Connectors 218
 - 8.11 Signal Conditioning Units 219
 - References 222
- 9 Calibration 223**
 - 9.1 Calibration Fundamentals 224
 - 9.1.1 Calibration Theory and Problems 224
 - 9.1.2 Mathematical Models 226
 - 9.1.3 Description of Interactions 229
 - 9.1.4 Tare Load Handling 233
 - 9.1.5 Asymmetric Sensitivity 236
 - 9.1.6 Verification and Accuracy 237
 - 9.1.7 Traceability 240
 - 9.1.8 Realignment 240

- 9.1.9 Signal Conditioning 241
- 9.2 Calibration Equipment 243
 - 9.2.1 Calibration Sleeve 243
 - 9.2.2 Weights 244
 - 9.2.3 Position Measurement Equipment 244
 - 9.2.4 Water Levels 245
 - 9.2.5 Inclinometers; Accelerometers 245
 - 9.2.6 Theodolite 245
 - 9.2.7 Laser Based Position Measurement 246
 - 9.2.8 Reference Load Cells 246
 - 9.2.9 Cantilevers 247
 - 9.2.10 Knife-Edge Bearings 248
 - 9.2.11 Ball-Socket Bearings 248
 - 9.2.12 Ball Bearings 248
 - 9.2.13 Flexures 248
- 9.3 Calibration Principles 249
- 9.4 Direct Manual Calibration 255
 - 9.4.1 Calibration Program 258
 - 9.4.2 Evaluation Process 262
- 9.5 Calibration Machines 264
 - 9.5.1 Indirect Automatic Calibration 264
 - 9.5.2 Direct Automatic Calibration 268
- References 271
- 10 Utilization of Balances in the Wind Tunnel 273**
 - 10.1 Rigging and Test Preparation 273
 - 10.2 Damping Systems 275
 - References 276

List of Figures

Fig. 1.1	Extract from Simmons' material testing apparatus patent document (HBM Hofmann)	3
Fig. 1.2	Prof. Ruge with a model of a containment vessel (HBM Hofmann)	3
Fig. 1.3	Photographs of early wire gauge and the patented strain gauge SR4 (with permission by Dr. Stockmann)	4
Fig. 1.4	Test rig of Lilienthal for airfoil testing	6
Fig. 1.5	Schematic picture of Eiffel's wind tunnel in Auteuil	7
Fig. 1.6	Eiffel's wind tunnel balance with model	7
Fig. 1.7	Schematic drawing of P. Wingham balance in his report from 1945	9
Fig. 2.1	Model reference point (red) and balance reference point (black)	12
Fig. 2.2	Calibration load cycle with hysteresis	18
Fig. 2.3	Definition of wind axis system in USA	19
Fig. 2.4	Definition of model axis system in Europe	19
Fig. 3.1	Half model balance test setup	24
Fig. 3.2	Half model balance	25
Fig. 3.3	External balance and support with a full model	25
Fig. 3.4	Schematic drawing of a weigh beam balance	27
Fig. 3.5	Load cell suspended weigh beam system	27
Fig. 3.6	Overhead balance with mechanical controlled weigh beams (TU Darmstadt)	28
Fig. 3.7	Principle design of a pyramidal balance	29
Fig. 3.8	Extended principle design of a pyramidal balance	30
Fig. 3.9	Three component pyramidal balance overhead on a small wind tunnel at the University of Wichita	30
Fig. 3.10	Principle design of a platform balance	31
Fig. 3.11	External platform balance of TU Darmstadt low speed wind tunnel	32

Fig. 3.12 Column balance of Kirsten wind tunnel; University of Washington 33

Fig. 3.13 Principle design of a column balance 33

Fig. 3.14 Sketch of Kirsten wind tunnel external balance 34

Fig. 3.15 Principle design of a yoke balance 35

Fig. 3.16 Yoke balance with centered balance reference point 36

Fig. 3.17 Yoke balance of DLR acoustic wind tunnel 36

Fig. 3.18 Spiral spring balance from Regensburg University of Applied Science wind tunnel 37

Fig. 3.19 Three flange external balance 38

Fig. 3.20 Internal sting balance for a cryogenic wind tunnel with double axial force section 39

Fig. 3.21 Force balance with tension transducers in forward and aft section 40

Fig. 3.22 Principles of a moment type balance 42

Fig. 3.23 Moment type balance 42

Fig. 3.24 Mono piece box balance 43

Fig. 3.25 Small box balance with load cells 44

Fig. 3.26 Vehicle fixed wheel load balance 44

Fig. 3.27 Compact floating frame balance (Carl Schenck Company Darmstadt) 45

Fig. 3.28 Principle of a compact external floating frame balance 46

Fig. 3.29 Six-component rotating balance (DNW, EADS) 46

Fig. 3.30 Axis system and temperature measurement locations on EADS/DNW rotating balance 47

Fig. 3.31 Rudder balance (change of angle of attack by different adapters) 47

Fig. 3.32 Missile balance built by Cassidian (Germany) for Eurofighter 49

Fig. 3.33 Missile balances of Cassidian (Germany) 49

Fig. 3.34 Electromagnetic force transducer 50

Fig. 4.1 Effect of lift on drag by an error in angle of attack 54

Fig. 4.2 Three-sting mounting on external balance 56

Fig. 4.3 Centre-strut mounting on external balance 56

Fig. 4.4 Semi-span model on external balance 57

Fig. 4.5 Wire supported model on overhead external balance 58

Fig. 4.6 Tail sting with fin attachment on lower side 59

Fig. 4.7 Tail sting through engine nozzle 59

Fig. 4.8 ETW twin sting rig 59

Fig. 4.9 Airbus model with fin sting mounting 60

Fig. 4.10 Anti-vibration system of ETW built by the ERAS Company, (Göttingen) 62

Fig. 4.11 Drawing of sting for balance W609 with cavities for pull-on screws and roll pin 66

Fig. 4.12 Cone connection with coupling nut and pin 67

Fig. 4.13	Cone connection with sleeve nut (threaded barrel, NASA)	68
Fig. 4.14	Slender cone with clamping keys	68
Fig. 4.15	Slender cone with expander clamping by NASA Langley Research Center	69
Fig. 4.16	Steep cone with conical center key lock	69
Fig. 4.17	Balance W614 with cylinder as model interface	70
Fig. 4.18	Model adapter for balance W614 with central hole for roll adjustment	71
Fig. 4.19	Cylinder shell mounting of a force balance	72
Fig. 4.20	Moment balance without and with mounted shell adapter	72
Fig. 4.21	Bloc-sting adapter of a balance with connector for prismatic mounting	73
Fig. 4.22	Bloc-model adapter with diagonal screws for mounting	74
Fig. 4.23	Flanges with keys for roll and lateral positioning (left), with centering for lateral and bolts for roll positioning (right), rotatable by 90° (right side)	74
Fig. 4.24	Balance interface with coupling nut and serration (<i>Hirth Tooth System</i>)	75
Fig. 4.25	Assumption of flange deformation to calculate maximum screw force	76
Fig. 4.26	Double hexagon high strength screws	76
Fig. 4.27	High capacity flange with center keys for positioning	77
Fig. 4.28	Conversion of sting balance from rear sting support to center strut support	79
Fig. 4.29	Conversion of box balance to rear sting mounting	79
Fig. 5.1	Wind axis system/model axis system	83
Fig. 5.2	a Half model on external balance. b Full model on external balance	84
Fig. 5.3	Load rhombus, load trapeze	89
Fig. 5.4	Specific load parameter of some balances	91
Fig. 5.5	Force and moment acting on a sleeve over the reference point	92
Fig. 6.1	Flowchart for balance calculation	105
Fig. 6.2	Measurement sections for forces and moments of a six-component balance	106
Fig. 6.3	Load reference point between section 1 and 2	108
Fig. 6.4	Load reference center placed at bending section 1	109
Fig. 6.5	Load reference center on model end of the balance	109
Fig. 6.6	Specific load parameter of some balances	111
Fig. 6.7	Moment distribution, stress and strain formulas	112
Fig. 6.8	Bending moment distribution by force, stress and strain formulas	112
Fig. 6.9	Torque moment distribution, stress and strain formulas	112
Fig. 6.10	Dimensions of a rectangular cross-section	114
Fig. 6.11	Dimensions for the octagonal cross-section	115

Fig. 6.12 Dimensions of a circular cross-section with flattenings 116

Fig. 6.13 Dimensions of a cruciform cross-section with fillets 118

Fig. 6.14 Approximation for cruciform cross-section with fillets 118

Fig. 6.15 Dimension for hexagonal cross-section on side 119

Fig. 6.16 Dimension for hexagonal cross-section on top 120

Fig. 6.17 Dimensions for rectangles with rib on the side 121

Fig. 6.18 Dimensions for rectangles with rib on top 122

Fig. 6.19 Cryogenic balance W612 for Cologne cryogenic wind tunnel 126

Fig. 6.20 Balance W610 for the TU Darmstadt low speed wind tunnel ... 126

Fig. 6.21 Cage bending section with five rectangular beams 128

Fig. 6.22 Deformation of cage by lateral forces 129

Fig. 6.23 Deformation of cage by M_y or M_z 130

Fig. 6.24 Deformation of the cage by rolling moment M_x 132

Fig. 6.25 Principle axial force system 134

Fig. 6.26 Nomenclature of a basic axial force system 134

Fig. 6.27 Flexure system of balance W621 139

Fig. 6.28 NLR balance with variation in flexure length and thickness 139

Fig. 6.29 Contours for a constant stress beam 140

Fig. 6.30 Two trapeze cantilever beams with constant stress zones (normal or orthogonal to the trapeze area) 141

Fig. 6.31 Coupled double trapeze axial force beam 142

Fig. 6.32 Temperature gradients by a sudden temperature change of 40 K 144

Fig. 6.33 Temperature gradient effect on the axial force system 144

Fig. 6.34 Conventional flexure system deformed by a temperature gradient 145

Fig. 6.35 Axial force system with double axial force element 146

Fig. 6.36 Sting balance for ETW with four constant stress axial force beams 147

Fig. 6.37 Calibration of temperature gradient influence 148

Fig. 6.38 Principal axial force element arrangement of ONERA 148

Fig. 6.39 Deformations of ONERA axial force elements design 149

Fig. 6.40 Temperature sensor arrangement to determine the gradient influence Eq. (6.147) 150

Fig. 6.41 Wiring scheme for temperature sensors to compensate gradient influence 150

Fig. 6.42 External balance turning options 152

Fig. 6.43 Balance platform deformation under vertical loads 153

Fig. 6.44 Load cell arrangement for external balance 154

Fig. 6.45 Yawing moment options 155

Fig. 6.46 Connecting rod with flexures 157

Fig. 6.47 Principle design of a semi-span balance with an example of gauge arrangement 158

Fig. 6.48 Possible cage arrangement in semi-span balances 159

Fig. 6.49 Semi-span balance 804S of NASA Langley, detailing the flexure design 160

Fig. 6.50 Cage design calculation axes, internal balance left, semi-span balance right 160

Fig. 6.51 Semi-span balance and flexure systems for the Cologne cryogenic wind tunnel 161

Fig. 6.52 Flexure system in X Axis Flexure system in Z Axis 162

Fig. 6.53 Stress in flexure by normal force F_z stress in flexure by axial force F_x 163

Fig. 6.54 Rectangular flexure with rib Trapeze flexure with rib 163

Fig. 6.55 Flange with serration and clamp Flange with crosswise keys and screws 164

Fig. 6.56 Deformation by temperature difference between top and bottom of the balance 164

Fig. 6.57 Assumptions for temperature gradients 165

Fig. 6.58 Error signal in the components due temperature gradients (case 1 to 6) 166

Fig. 6.59 Slotted flange Basic shape cross 167

Fig. 6.60 Semi-span balance integration to model support of KKK 168

Fig. 6.61 Axial force of wires with temperature change 168

Fig. 6.62 ETW balance with additional wires and tubes glued in surface slots 169

Fig. 6.63 Principle semi-span test setup with turbine power simulator at Aircraft Research Association (UK) 170

Fig. 6.64 Airline bridge on DNW-LLF balance (DNW, Airbus) 171

Fig. 6.65 Typical Wöhler diagram with lifetime regions 172

Fig. 6.66 Wöhler curve with stress collective for Miner Rule 175

Fig. 7.1 Integration of heat treatment into manufacturing process for Maraging steel 182

Fig. 7.2 Welded balance, parts and complete body after welding 188

Fig. 8.1 Relative resistance change of N-type-gauges versus strain 191

Fig. 8.2 Relative resistance change of P-type gauge versus strain 192

Fig. 8.3 Apparent strain of P-Type semiconductor gauges on different materials (Vishey Micro Measurements) 193

Fig. 8.4 Apparent strain of a compensated N-Type semiconductor gauge on Al 2024 (Vishey Micro Measurements) 194

Fig. 8.5 Principle of Fabry-Pérot strain gauge 195

Fig. 8.6 Wavelength distribution of fiber Bragg strain gauges, blue = strong reflecting, red = weak reflecting (HBM) 196

Fig. 8.7 Example scheme of bonding pressure calibration 201

Fig. 8.8 Wheatstone bridge circuit 201

Fig. 8.9 Wheatstone bridge with circuit wire resistors 204

Fig. 8.10 Lead wire connection points 205

Fig. 8.11 Zero output compensation with constantan resistors 207

Fig. 8.12 Typical apparent strain curve of a strain gauge (Vishey) 208

Fig. 8.13	Balance zero drift with matched gauges	208
Fig. 8.14	Poisson gauge bridge compensation for different temperatures in two areas	209
Fig. 8.15	Cantilever beam as force transducer	211
Fig. 8.16	Gauge factor shift of Karma and constantan (Vishey)	212
Fig. 8.17	Wheatstone bridge with sensitivity shift compensation	213
Fig. 8.18	Wiring scheme for force and moment of a direct read balance	215
Fig. 8.19	Wiring scheme for force and moment on a moment balance	216
Fig. 8.20	Poisson bridge with a nitrile rubber coating	217
Fig. 8.21	Cryogenic balance coated by CVD with silicon carbide	218
Fig. 9.1	Approximation of third-order function (top) and inverse third-order function	227
Fig. 9.2	Third-order approximation of calibration data and approximation error	228
Fig. 9.3	Side force interaction	231
Fig. 9.4	Product interaction of F_x and F_z	232
Fig. 9.5	Calibration curve and error diagram	233
Fig. 9.6	Errors due to non-linearity and tare loads	233
Fig. 9.7	Third-order characteristic with zero load shift	234
Fig. 9.8	Implementation of absolute value terms	235
Fig. 9.9	Transducer section of finite-element model of a typical able balance	237
Fig. 9.10	Possible resolution versus bandwidth for 10 and 20 V excitation (HBM)	242
Fig. 9.11	Linking rod under compression	246
Fig. 9.12	Types of flexures a orthogonal separated; b Cardan joint (Ormond); c swivel joint (Riverhawk Co.)	249
Fig. 9.13	Direct calibration principle	250
Fig. 9.14	Indirect calibration principle	252
Fig. 9.15	Direct calibration manual calibration	253
Fig. 9.16	Direct calibration with automatic load generation	253
Fig. 9.17	Calibration of a half-model balance on the external wind tunnel balance in the TU Darmstadt low speed wind tunnel	254
Fig. 9.18	Indirect automatic calibration	254
Fig. 9.19	TU Darmstadt balance calibration machine	255
Fig. 9.20	Manual calibration rig	256
Fig. 9.21	Balance support	256
Fig. 9.22	Bell crank for horizontal loading	257
Fig. 9.23	Calibration sleeve	258
Fig. 9.24	Flowchart of loading sequences	261
Fig. 9.25	Visual matrix	263
Fig. 9.26	Visual error matrix	263
Fig. 9.27	TU Darmstadt machine in operation mode	266
Fig. 9.28	Pneumatic force generator	266

Fig. 9.29	Master calibration setup of the TU Darmstadt machine	267
Fig. 9.30	Direct calibration using single vector principle of NASA Langley	269
Fig. 9.31	IAI automatic balance calibration system (ABCS)	270
Fig. 10.1	Flow chart for balance use in wind tunnel test campaigns	274
Fig. 10.2	Sting damping system of TU Darmstadt low speed wind tunnell	275
Fig. 10.3	ETW sting integrated anti-vibration system (ERAS company, Göttingen)	276

List of Tables

Table 2.1	Definition of positive axis direction	20
Table 2.2	Wind tunnel standards	21
Table 4.1	Example cones used in different balances	65
Table 4.2	Major characterising features of balance joints	78
Table 4.3	Balance interface characteristics	78
Table 5.1	Maximum combined loads for external balance	86
Table 5.2	Determination of maximum combined load for an internal balance	87
Table 5.3	Nomenclature “Allowed Uncertainty”	97
Table 5.4	Typical value ranges for the uncertainty factors	97
Table 7.1	Balance body material properties at ambient temperature	179
Table 7.2	List of maraging steels used by TU Darmstadt	181
Table 7.3	High strength stainless steels	183
Table 8.1	Parameters used in defining sensitivity of FBGS sensors in Eq. (8.10)	196
Table 8.2	Quantities of equation (8.34)	213

Chapter 1

Historical Review



1.1 Introduction

Before embarking on a detailed description of wind tunnel balance design, it is instructive to first review the evolution of force measurements using such balances. The justification for such a review in an engineering handbook is quite simple and comes from years of experience.

Despite having access to innumerable articles written on a subject, the chronological sequence of these articles can be particularly revealing about why and when certain inventions were made. Circumstance often lies behind the saying that 'necessity is the mother of invention'. This is very well exemplified by the parallel development of two sectors eventually merging to yield what we now know as strain gauge based wind tunnel balances. On the one hand very basic physical laws and effects of elasticity and electricity were being developed, eventually culminating in the fundamentals of measuring strain with a strain gauge. On the other hand, the need for aerodynamic force measurements was rising rapidly with the advent of wind tunnel testing. It is this sequence of events and steps of progress which is summarized in the following sections.

1.2 From Fundamental Physics to the First Force Transducers

The basic research to build a force transducer with a metal spring and a wire strain gauge was conducted by *Robert Hooke* (1635–1703), *Georg Simon Ohm* (1789–1854), *Charles Wheatstone* (1802–1875) and *William Thomson, 1st Baron Kelvin of Largs* (1824–1907).

Robert Hooke was a famous physicist and an architect. Among other things he formulated in 1678 the basic theory of elasticity [9] and this is also the reason why the elastic relationship between stress and strain is known as *Hooke's Law*.

Georg Simon Ohm was professor for physics at the universities of Cologne, Nuremberg and Munich. In 1827 he published his work on the correlation between voltage, current and electrical resistance. His relation between voltage current and resistance became the basic principle for an electrical circuit and the measurement of electrical resistance [16]. Using his name as the unit for the electrical resistance honored this work.

Charles Wheatstone contributed work on the electrical telegraph and published work on the “*Wheatstone Bridge*” circuit in 1843 [22]. Although he never claimed to have invented the special electric circuit to determine small electrical resistances that was named after him. The first description of the bridge circuit was given by *Samuel Hunter Christie* (1784–1865), from the Royal Military Academy, who published it in 1833 [4].

William Thomson was knighted in 1866 and became *1st Baron Kelvin of Largs* in 1892. His most famous works were his contributions that made the first transatlantic telegraph cable a success, but he also published numerous articles on physics, among these in 1856 an article on the relationship between mechanical stress and electrical resistance of metals [21], which had been already mentioned by *Wheatstone*.

This small excursion to early developments shows, that the basics for metal strain gauges resulted from the work of several scientists working sequential to one another with only minimal temporal overlap. For instance, after *Thomson’s* contribution, another 61 years went by until the first use of the effect was reported for a sensor application. The first person who actually used the effect of the change of electrical resistance under mechanical stress for measurements was *Walther Nernst* (1864–1941), who built a pressure gauge in 1917 to measure the pressure fluctuations inside a piston engine. This application, and the resulting pressure diagram were published in 1928 [12, 13].

Edward. E. Simmons (1911–2004) was an assistant at the *California Institute of Technology* when he invented a material testing apparatus for measuring the percussive force in 1936. At that time *Simmons* and others he worked with probably did not realize the importance of their invention and that is one reason that it was patented only several years later [19, 20]. The patent for this apparatus [17] was granted in 1942 (Fig. 1.1). This is the first application where a wire strain gauge was used to measure a force.

At nearly the same time on the east coast at *Massachusetts Institute of Technology*, *Arthur Claude Ruge* (1905–2000) used a meandering wire on a piece of paper to measure the strain on the surface of a containment vessel model to predict the stresses in the real vessel (Fig. 1.2). This was the first use of a resistance strain gauge in experimental stress analysis.

The aerospace industry was developing an urgent need for simple and inexpensive strain measurement sensors at that time and so the first industrially produced foil strain gauge, **SR4**, immediately became a success. The sensor was named **SR4** because *Simmons* and *Ruge* together with four people (*de Forest, Tatnall, Clark and Hathaway*) negotiated the terms of the corporate patent of *Simmons* and *Ruge* for the wire strain gauge.

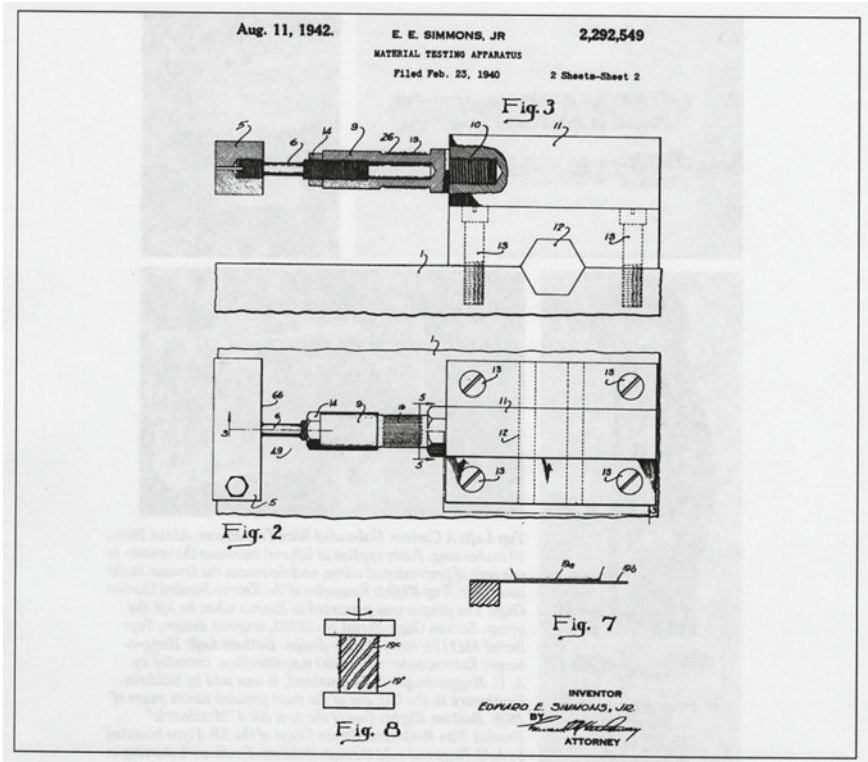
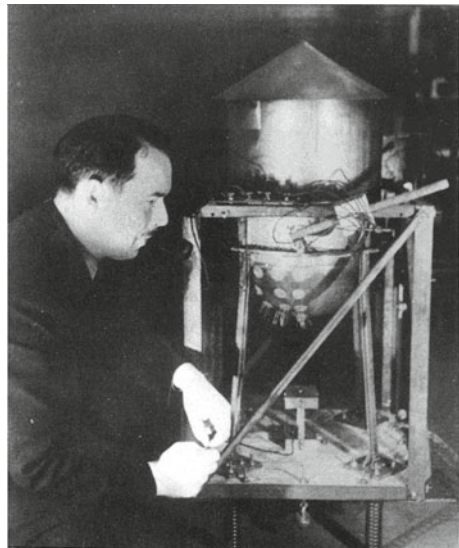


Fig. 1.1 Extract from Simmons' material testing apparatus patent document (HBM Hofmann)

Fig. 1.2 Prof. Ruge with a model of a containment vessel (HBM Hofmann)



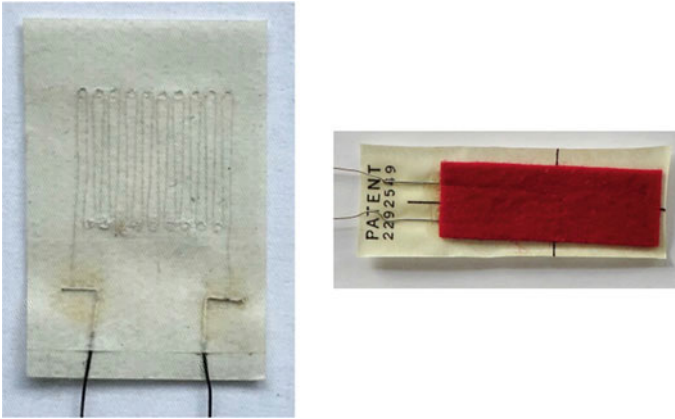


Fig. 1.3 Photographs of early wire gauge and the patented strain gauge SR4 (with permission by Dr. Stockmann)

The success story of the metal strain gauge was described by *Tatnall* [8]. He was a salesman of the *Baldwin-Southwark Company* and promoted the distribution of the paper strain gauges produced by the *Ruge/de Forest Company*, so that the planned production for the first year (1941) of 50,000 gauges (Fig. 1.3) was sold out within two months. The Second World War and the associated rapidly expanding aircraft industry created great demand for these strain gauges for material testing and testing of aircraft structures. The paper strain gauge dominated the area of experimental stress analysis very rapidly. The strain gauge production company of *Ruge and de Forest* was sold to *Baldwin Lima Hamilton (BLH)* in 1955, a company which today still produces gauges designated **SR4**.

In the field of force measurement some developments can be traced back to the beginning of the 20th century using electro dynamometers as force transducers. In the USA *Burton McCollum* and *O.S. Peters* published an article about a “new electrical telemeter” in 1924 [15]. They used a stack of carbon plates as a strain sensitive element and so, were the first to use a semiconductor gauge for strain measurement. Another example was a piezoelectric dynamometer that was used in a test by *Max Kramer* at the *Aachen University of Technology* in 1932 to determine the dynamic lift force of a two-dimensional wing generated by a quick change of angle of attack [14]. In 1932 *Fred Scoville Eastman* from the *University of Washington* reported on a weigh beam for an external balance using an electromagnetic dynamometer [6].

All of these applications were used or proposed for use in a wind tunnel, but eventually metal strain gauge sensors dominated this application for wind tunnel strain gauge balances. One main reason for this was the next significant step in the development of the strain gauges made by *P. Jackson* in Great Britain with the invention of the foil strain gauge, where the grid was no longer a wire [10]. The production of the gauge was performed using a photo-chemical etching process, similar to that of the printed circuit technology by the *Technograph Inc. Company*

under the license of the *Saunders-Roe Company (UK)* in 1952, where *P. Jackson* worked as a test engineer.

This process resulted in the mass production of the gauges, which made high quality gauges much less expensive and more reliable. In 1954 the *Baldwin Company* bought the license for the production of foil strain gauges from *Technograph Inc. (UK)* and the *SR-4 foil strain gauge* was produced.

In the 1950s several companies emerged to produce strain gauges in large numbers and in increasingly varied shapes. *Hottinger Messtechnik* started production of foil strain gauges in Darmstadt in 1955 [11] and in 1963 this company merged with *Baldwin Lima Hamilton Corp.* and formed *Hottinger Baldwin Messtechnik (HBM)*. *HBM* still exists today, but is now owned by other companies. Since 2001 *BLH* is part of the *Vishay Company*, which was founded at the beginning 1960s and is now the largest strain gauge manufacturer worldwide. Numerous other strain gauge manufacturers were established over the years, but none of these play a role in the market comparable to *BLH*, *HBM* and *Vishay Micro Measurements*.

Up to now in this historical review the story of the semiconductor strain gauges was not mentioned. One reason for this is that semiconductor strain gauges do not play a major role in the production of wind tunnel balances. This is because of their nonlinear characteristic and their strong temperature sensitivity. However, for some applications they are applicable, where a quick response to a sudden or dynamic change in load must be measured. Then their high sensitivity and the likely higher stiffness of the balance body are decisive. Semiconductor strain gauges use the piezoresistive effect, the change of the electrical resistance caused by the change of density in the crystal structure of a semiconductor under stress. *P.W. Bridgman* conducted comprehensive experiments on the electrical resistance of metals and crystals and in 1932 he published an article on the effect of homogeneous mechanical stress on the electrical resistance of a crystal [3]. He tested the change of resistance on crystals by the influence of static pressure. Under his supervision *Mildred Allen* performed first experiments on the effect of tension on crystals in 1932 [1]. She tested the change of electrical resistance on Bismuth crystals under tension, related to different crystal orientations. However, her measurements did not directly lead to the development of a strain sensor.

About 20 years later *Charles S. Smith* at the *Bell Laboratories* discovered the strain sensitivity of Germanium and Silicon. This research was used to develop the semiconductor strain gauge [18]. In 1958 *Honeywell* offered the first commercially produced semiconductor strain gauge [18]. In the coming years numerous developments arose using semiconductor strain gauges for pressure transducers (*Kulite*, *Honeywell*). Since 1962 *Baldwin Lima Hamilton (BLH)* has offered bondable semiconductor strain gauges, similar in use to the metal strain gauges they produce. However productions of these strain gauges was terminated some years ago. The use of bonded semiconductor strain gauges was described in detail by *James Dorsey* from *BLH* in his *Semiconductor Strain Gage Handbook* [5] in 1964 and *BLH* offered semiconductor strain gauges until 2004. Nowadays, semiconductor strain gauges are available from *Kulite*, *Kyowa* and *Micron Instruments*.

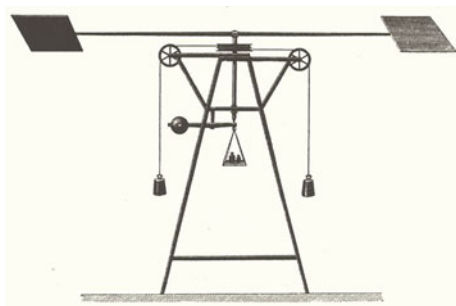
1.3 Force Measurement in Wind Tunnels

Apart from the development of strain gauges, there was also the development of force transducers and wind tunnel balances. With the acceleration of aerodynamic research and the use of wind tunnels in the early 20th century, the measurement of aerodynamic forces on test specimens was of paramount importance.

Benjamin Robins (1707–1751) and later on in 1804 *Sir George Cayley* were the first to perform experiments with a whirling arm to determine lift on plate segments [2]. Also *Otto Lilienthal*, around 1888, used a whirling arm apparatus to obtain lift and drag for different profiles (Fig. 1.4). Lift was measured by the weights, which balanced the thrust of the “propeller” and the drag was proportional to the time which the weights needed to reach the ground. The disadvantages of such a system are obvious. There are only short or no moments with steady state conditions during the experiment. This is likely one of the reasons why *Frank H. Wenham* (1824–1908) built a wind tunnel in 1871, which used a steam engine to drive a fan upstream of the model to generate a constant airflow through a wooden box of 3.7 m length and a cross section of 45 cm × 45 cm. This wind tunnel is the first documented wind tunnel and it was built for the Royal Aeronautical Society. It is reported that *Wenham* used a device to measure the forces on profiles by compensating the forces with weights outside the tunnel section. This device looked like a balance which was usually used to measure weight, and so the designation “Wind Tunnel Balance” may be traced back to this force measuring instrument. Later on the *Wright Brothers* employed a small wind tunnel with an external balance for their experiments with airfoils.

One of the first larger wind tunnels in which experiments with models of airplanes were conducted was built by *Gustave Eiffel* in 1910 [7]. His principle of a flow-through wind tunnel, sucking air through a nozzle, test section, collector and a diffuser with a fan drive at the end of the diffuser, is still in use today and tunnels built according to this design are called *Eiffel* type wind tunnels (Fig. 1.5). He also used an external wind tunnel balance according to the compensation principle (Fig. 1.6). So the use of external balances, working according to the compensation principle, prevailed as the wind tunnel force measurement system.

Fig. 1.4 Test rig of Lilienthal for airfoil testing



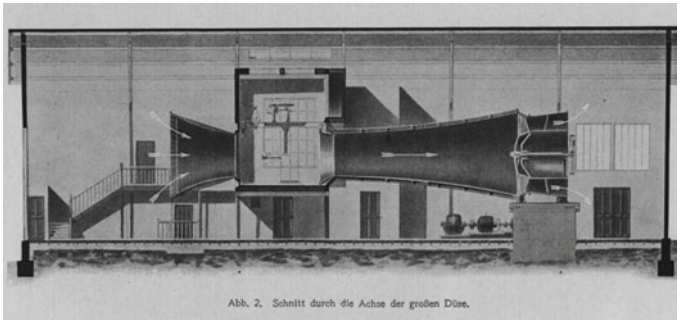
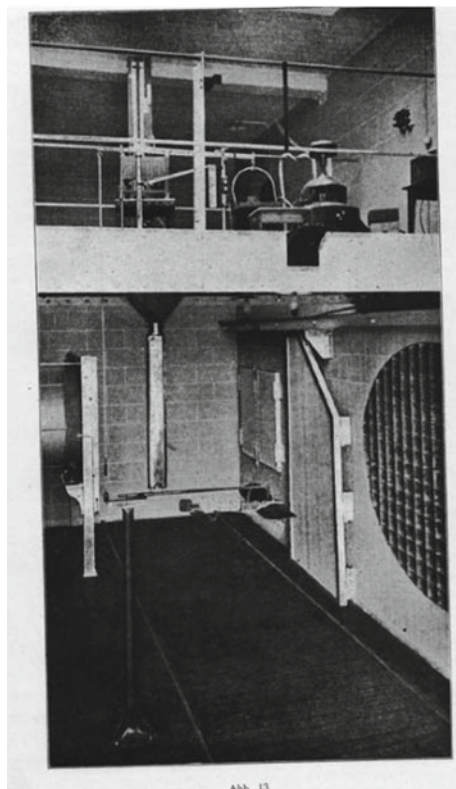


Fig. 1.5 Schematic picture of Eiffel's wind tunnel in Auteuil

Fig. 1.6 Eiffel's wind tunnel balance with model



As remarked above, some key developments took place in the early 1930s and in the mid 1940s, when electrical sensor based force transducers were used to measure dynamic forces in a wind tunnel, or in the first pressure transducer of *Nernst*. However the real breakthrough for transducer based force measurements in a wind tunnel was the invention of the strain gauge. It is understandable that scientists and the engineers immediately adopted this inexpensive and precise sensor for the development of force transducers. The high sensitivity of the strain gauge allowed the development of force transducers with a very high stiffness and precision.

In all countries with an aircraft industry, numerous wind tunnels were being built. These tunnels required precise, multi-component force measurements. Following the Second World War a large number of high *Mach* number tunnels were also built. To achieve high *Reynolds* numbers at supersonic speed these tunnels were pressurized and the model loads increased, caused by the higher density of the gas. This circumstance, and the relatively low interaction afforded using a back sting support, made the development of the compact sting balance necessary and the development of the internal sting balance was only possible by using strain gauges.

The first report of such an internal sting balance is the report of Wingham [23] from 1945. *Wingham* used strain gauges to measure lift and pitch on a model in a high-speed wind tunnel. This balance was a sting balance with two bending sections (Fig. 1.7).

In this report a reference to an earlier report from 1944 by members of *Vickers-Armstrong Ltd.* was mentioned, but this report was not published. Thus, although it is not absolutely clear who and when the first sting strain gauge balance was built, it is clear that shortly after the strain gauge was commercially available, wind tunnel engineers started to design and build wind tunnel balances using strain gauges as sensors. In the early 1950s numerous developments in the area of sting balances and external balances with force transducers are reported. Along with the construction of new wind tunnels, the development of new balances was necessary to achieve precise and reliable results for the aerodynamic force measurement.

After a long period of development, the emergence of cryogenic wind tunnels (around 1980) set new requirements for the temperature stability of internal wind tunnel balances. The balances for these tunnels were required to measure with the precision of balances at ambient temperature, but over a much larger temperature range. Without this precision, the advantage of the high *Reynolds* number achieved using the cryogenic temperatures was useless. The challenges generated by the cryogenic wind tunnels were responsible for the latest developments of strain gauge based wind tunnel balances.

Optical strain gauges with higher sensitivity than the metal foil gauges did not have a major impact on the development of the wind tunnel balances. Their capabilities can only be fully exploited when new balance materials with a much higher *Young's modulus* than that of steel are available.